Congestion on Multilane Highways

September 4, 2001

J. M. Greenberg[1]
A. Klar[2]
M. Rascle[3]

Abstract

On the multilane freeways one often observes distinct stable equilibrium relationships between auto velocity and density. Prototypical situations involve two equilibria

$$v = v_1(\rho) > v = v_2(\rho) \quad , \quad 0 \le \rho < \rho_{\max}$$

where $v_1(\cdot)$ and $v_2(\cdot)$ are monotone decreasing and satisfy $v_1(\rho_{\max}) = v_2(\rho_{\max}) = 0$. The upper curve is typically stable for densities satisfying $0 \le \rho \le \rho_1$ whereas the lower curve is stable for densities satisfying $\rho_2 \le \rho \le \rho_{\max}$. Our interest is in the situation where $0 < \rho_2 \le \rho_1 < \rho_{\max}$ and $v_2(\rho_2) \le v_1(\rho_1)$.

In this paper we present a model which incorporates both equilibrium curves and a simple switching mechanism which allows drivers to transition from one equilibrium curve to the other. What we observe with this model are relaxation oscillations seen in congested traffic; i.e. periodic waves separating fast and slow moving traffic which propagate upstream.

1 Introduction

On the multilane freeways one often observes distinct stable equilibrium relationships between auto velocity and density. Prototypical situations involve two equilibria

$$v = v_1(\rho) > v = v_2(\rho) \quad , \quad 0 \le \rho < \rho_{\max} \tag{1.1}$$

[1]Department of Mathematical Sciences, Carnegie Mellon University, Pittsburgh, PA, USA. This research was partially supported by the Applied Mathematical Sciences Program, U. S. Department of Energy and the U. S. National Science Foundation. (greenber@andrew.cmu.edu)

[2]FB Mathematik, TU Darmstadt, Germany. This research was partially supported by the German research foundation (DFG). (klar@mathematik.tu-darmstadt.de)

[3]Mathematiques, Univ. of Nice, France (rascle@math.unice.fr)

where $v_1(\cdot)$ and $v_2(\cdot)$ are monotone decreasing and satisfy $v_1(\rho_{\max}) = v_2(\rho_{\max}) = 0$. The upper curve is typically stable for densities satisfying $0 \le \rho \le \rho_1$ whereas the lower curve is stable for densities satisfying $\rho_2 \le \rho \le \rho_{\max}$. Our interest is in the situation where $0 < \rho_2 \le \rho_1 < \rho_{\max}$ and $v_2(\rho_2) \le v_1(\rho_1)$.

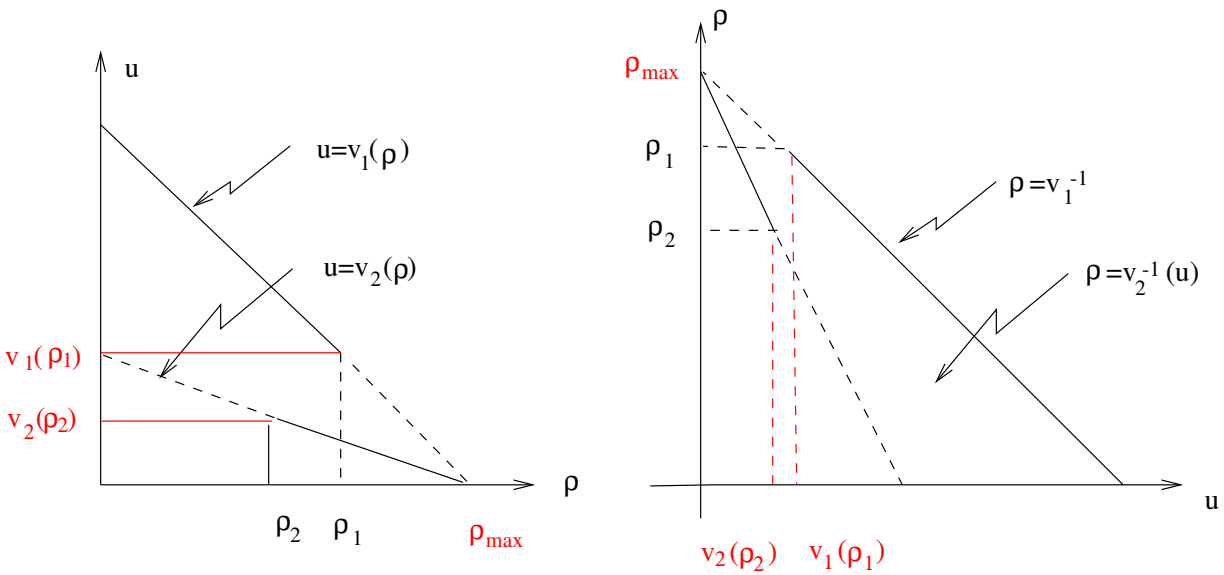

Figure 1

The explanation for the two curves is quite simple. For high density congested traffic lane changing and passing is difficult and dangerous and this yields the slower equilibrium curve. On the other hand, when the traffic is less dense, lane changing and passing becomes easier and this yields the faster equilibrium curve.

In this paper we present a model which incorporates both equilibrium curves and a simple switching mechanism which allows drivers to transition from one equilibrium curve to the other. What we observe with this model are relaxation oscillations seen in congested traffic; i.e. periodic waves separating fast and slow moving traffic which propagate upstream.

Our basic descriptors are the car density ρ (in units of cars/mile) and velocity u (in units of miles/hour). We also track

$$\alpha = u - v_1(\rho)$$

which represents the discrepancy between the actual car speed and the uncongested maximum speed.

Our governing equations are

$$\frac{\partial \rho}{\partial t} + \frac{\partial}{\partial x}(\rho u) = 0 \tag{1.2}$$

and

$$\frac{\partial \alpha}{\partial t} + u\frac{\partial \alpha}{\partial x} = \begin{cases} \dfrac{-\alpha}{\epsilon} & , \quad \rho < R(u) \\ \dfrac{((v_2 - v_1)(\rho) - \alpha)}{\epsilon} & , \quad \rho \geq R(u). \end{cases} \tag{1.3}$$

Here, $u \to R(u)$ is a monotone non-decreasing function satisfying

$$R(u) = \rho_2 \quad , \quad 0 \leq u \leq v_2(\rho_2) \text{ and } R(u) = \rho_1, \ v_1(\rho_1) \leq u. \tag{1.4}$$

For experimental data and the choice of the switch curve we refer to the work of B. Kerner [6, 7]. In his thesis, Sopasakis [1] gave an argument supporting the choice $\rho_2 = \rho_1$ and $R(u) \equiv \rho_2, \ 0 \leq u$.

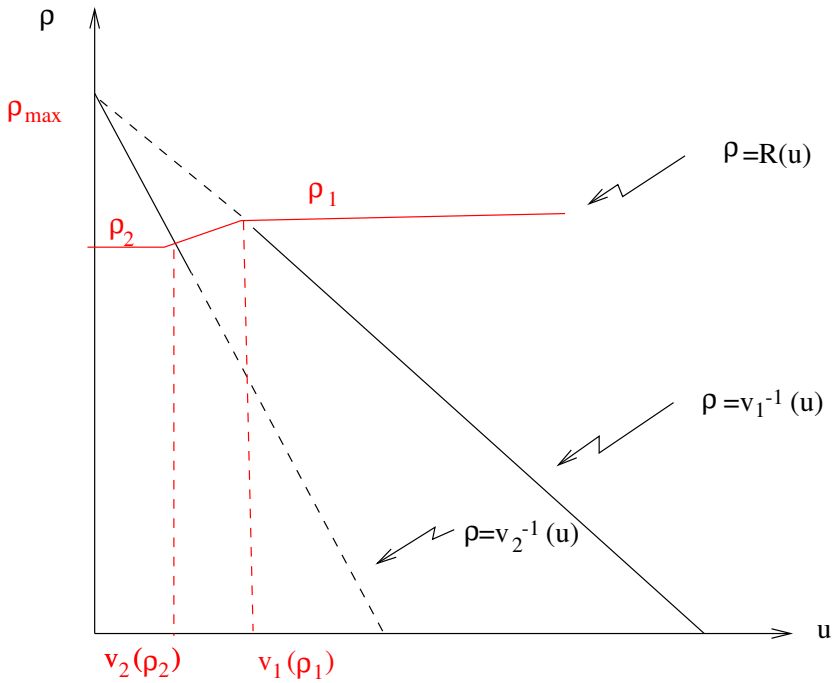

Figure 2

Equations (1.2) and (1.3) imply that u satisfies

$$\frac{\partial u}{\partial t} + (u + \rho v_1'(\rho))\frac{\partial u}{\partial x} = \begin{cases} \dfrac{v_1(\rho) - u}{\epsilon} & , \quad \rho < R(u) \\ \dfrac{v_2(\rho) - u}{\epsilon} & , \quad \rho \geq R(u). \end{cases} \tag{1.5}$$

For $0 < \rho \leq \rho_{\max}$, the system (1.2), (1.4), and (1.5) is strictly hyperbolic with distinct wave speeds $c_1 = u + \rho v_1'(\rho) < c_2 = u$. Variants of this relaxation model with one

equilibrium and no switch curve have been studied by Aw and Rascle [2], Greenberg et. al [3,4], and Aw, Klar, Materne, and Rascle [5]. The principal results of those investigations relevant to us here are that for any initial data $\rho_0(\cdot)$ and $u_0(\cdot)$ satisfying

$$0 \le u_0(x) \le v_1(\rho_0(x)) \text{ and } 0 \le \rho_0(x) \le \rho_{\max} \tag{1.6}$$

the system (1.2), (1.4) and (1.5) has an appropriately defined weak solution satisfying (1.6) for all future times. Thus the model presented here has no signals propagating faster than the car velocities and yields none of the velocity reversals seen in the Payne-Whitham models. These two observations are the basic strength of this class of second order model.

For simplicity we restrict our attention to spatially periodic solutions – the ring road scenario. We shall also work with a Lagrangian reformulation of the system. When discretized this Lagrangian system yields a follow-the-leader type model.

We let l be the spatial period of our data $\rho_0(\cdot) > 0$ and assume that

$$\int_0^l \rho_0(\xi)d\xi = M \tag{1.7}$$

is an integer. For any real number $m \in [0, M]$ we let $x^0(m)$ be the unique solution of

$$m = \int_0^{x^0(m)} \rho_0(\xi)d\xi \tag{1.8}$$

and $x(m,t)$ be the solution of

$$\frac{\partial x}{\partial t}(m,t) = \bar{u}(m,t) \stackrel{def}{=} u(x(m,t),t) \text{ and } x(m,0) = x^0(m). \tag{1.9}$$

Here, ρ and u are solutions of (1.2), (1.4) and (1.5). The continuity equation (1.2), when combined with (1.8) and (1.9) yields

$$m = \int_{x(0,t)}^{x(m,t)} \rho(\xi,t)d\xi \tag{1.10}$$

and (1.10) in turn implies that

$$\bar{\rho}(m,t) \stackrel{def}{=} \rho(x(m,t),t) \text{ and } \bar{\gamma}(m,t) \stackrel{def}{=} \frac{\partial x}{\partial m}(m,t) \tag{1.11}$$

satisfy

$$\bar{\rho}(m,t)\bar{\gamma}(m,t) \equiv 1. \tag{1.12}$$

Additionally (1.9) implies that $\bar{\gamma}$ and $\bar{u}$ satisfy

$$\frac{\partial \bar{\gamma}}{\partial t}(m,t) = \frac{\partial \bar{u}}{\partial m}(m,t). \tag{1.13}$$

Finally, if we let

$$\bar{\alpha}(m,t) \stackrel{def}{=} \alpha(x(m,t),t) = \bar{u}(m,t) - V_1(\bar{\gamma}(m,t)), \tag{1.14}$$

then (1.3) implies

$$\frac{\partial \bar{\alpha}}{\partial t}(m,t) = \begin{cases} -\dfrac{\bar{\alpha}(m,t)}{\epsilon} & , \ \bar{\gamma}(m,t) > \dfrac{1}{R(\bar{u}(m,t))} \\ \dfrac{((V_2 - V_1)(\bar{\gamma}(m,t)) - \bar{\alpha}(m,t)}{\epsilon} & , \ \bar{\gamma}(m,t) \leq \dfrac{1}{R(\bar{u}(m,t))} \end{cases} \tag{1.15}$$

where

$$V_1(\bar{\gamma}) \stackrel{def}{=} v_1(1/\bar{\gamma}) \ \text{ and } \ V_2(\bar{\gamma}) \stackrel{def}{=} v_2(1/\bar{\gamma}). \tag{1.16}$$

In what follows we assume the functions $V_1(\cdot)$ and $V_2(\cdot)$ defined in (1.16) are increasing and concave on $[L \stackrel{def}{=} 1/\rho_{\max}, \infty)$ and satisfy

$$0 = V_2(L^+) = V_1(L^+) \ \text{ and } \ 0 < V_2^{(p)}(\bar{\gamma}) < V_1^{(p)}(\bar{\gamma}) \text{ for } L < \bar{\gamma} < \infty \text{ and } p = 0, 1 \tag{1.17}$$

and the limit relations

$$\lim_{\bar{\gamma} \to \infty} (V_i(\bar{\gamma}), \ V_i^{(p)}(\bar{\gamma})) = (v_i^{\infty}, 0), i \text{ and } p = 1, 2 \tag{1.18}$$

where $v_2^{\infty} < v_1^{\infty}$. The parameter L has the interpretation of the length of a typical car on the roadway.

Equations (1.13) - (1.15) also combine to give

$$\frac{\partial \bar{u}}{\partial t}(m,t) - V_1'(\bar{\gamma}(m,t))\frac{\partial \bar{u}}{\partial m}(m,t) = \begin{cases} \dfrac{V_1(\bar{\gamma}(m,t)) - \bar{u}(m,t)}{\epsilon} & , \ \bar{\gamma}(m,t) > \dfrac{1}{R(\bar{u}(m,t))} \\ \dfrac{V_2(\bar{\gamma}(m,t)) - \bar{u}(m,t)}{\epsilon} & , \ \bar{\gamma}(m,t) \leq \dfrac{1}{R(\bar{u}(m,t))}. \end{cases} \tag{1.19}$$

The Follow-the-Leader Model

In [3] Greenberg showed that for the Lagrangian system (1.9) - (1.19) the appropriate stable spatial differencing scheme was downwind. Moreover, such differencing, with $\Delta m = 1$ (recall cars are discrete), yields

$$\frac{dx_m}{dt} = \bar{u}_m, \tag{1.20}$$

$$\bar{\gamma}_m = x_{m+1} - x_m, \tag{1.21}$$

$$\bar{\rho}_m = \frac{1}{\bar{\gamma}_m}, \tag{1.22}$$

and

$$\begin{aligned} &\frac{d\bar{u}_m}{dt} - V_1'(x_{m+1} - x_m)(\bar{u}_{m+1} - \bar{u}_m) \\ &= \begin{cases} \dfrac{V_1(x_{m+1} - x_m) - \bar{u}_m}{\epsilon} & , \quad x_{m+1} - x_m > \dfrac{1}{R(\bar{u}_m)} \\ \dfrac{V_2(x_{m+1} - x_m) - \bar{u}_m}{\epsilon} & , \quad x_{m+1} - x_m \leq \dfrac{1}{R(\bar{u}_m)}. \end{cases} \end{aligned} \tag{1.23}$$

This latter system implies that

$$\bar{\alpha}_m \stackrel{def}{=} \bar{u}_m - V_1(x_{m+1} - x_m) \tag{1.24}$$

satisfies

$$\frac{d\bar{\alpha}_m}{dt} = \begin{cases} -\dfrac{\bar{\alpha}_m}{\epsilon} & , \quad x_{m+1} - x_m > \dfrac{1}{R(\bar{u}_m)} \\ \dfrac{((V_2 - V_1)(x_{m+1} - x_m) - \bar{\alpha}_m)}{\epsilon} & , \quad x_{m+1} - x_m \leq \dfrac{1}{R(\bar{u}_m)}. \end{cases} \tag{1.25}$$

These equations hold for $1 \leq m \leq M$ and $x_{M+1}(t) = x_1 + l$ where again l is the spatial period of our original data $\rho_0(\cdot)$ and $u_0(\cdot)$. The initial positions of the cars are constrained to satisfy

$$x_{m+1}(0) - x_m(0) \geq L \stackrel{def}{=} \frac{1}{\rho_{\max}} \tag{1.26}$$

and these numbers are related to $\rho_0(\cdot)$ by

$$\int_{x_m(0)}^{x_{m+1}(0)} \rho_0(\xi) d\xi \stackrel{def}{=} \bar{\rho}_m^0 (x_{m+1}(0) - x_m(0)) = 1. \tag{1.27}$$

In section 2 we analyze a first-order integration scheme for the system (1.20) - (1.22), (1.24), and (1.25). We obtain estimates which guarantee that

$$L \leq x_{m+1}(t) - x_m(t) \quad \text{and} \quad 0 \leq u_m(t) \leq V_1(x_{m+1}(t) - x_m(t)) \tag{1.28}$$

for all $t \geq 0$. These estimates guarantee the consistency of the model. In Section 3 we present some simulations with the discrete model. Here we see the persistent periodic wave trains separating congested regions of slow moving traffic from regions of less dense faster moving traffic. The waves separating these regions are analyzed in Section 4. In that section we revert to continuum model (1.9) and (1.11) - (1.19) because it is analytically easier to work with.

2 A Priori Estimates

In this section we establish a-priori estimates for solutions of (1.20) - (1.22), (1.24) and (1.25). We integrate these equations with a first-order Euler Scheme. Specifically, we let Δt be our time step, $t_n = n\Delta t$, and for any function $f_m(\cdot)$ we let f_m^n denote the approximate value of $f_m(\cdot)$ at t_n. Our integration scheme is

$$x_m^{n+1} = x_m^n + \Delta t u_m^n, \tag{2.1}$$

$$\bar{\gamma}_m^{n+1} = x_{m+1}^{n+1} - x_m^n, \tag{2.2}$$

$$\bar{\rho}_m^{n+1} = \frac{1}{\left(x_{m+1}^{n+1} - x_m^{n+1}\right)}, \tag{2.3}$$

$$\bar{\alpha}_m^{n+1} = \left(\bar{u}_m^{n+1} - V_1(x_{m+1}^{n+1} - x_m^{n+1})\right), \tag{2.4}$$

where

$$\bar{\alpha}_m^{n+1} = (1 - \Delta t/\epsilon)\,\bar{\alpha}_m^n + \Delta t(V_2 - V_1)(x_{m+1}^n - x_m^n)H\left(\bar{\rho}_m^n - R(\bar{u}_m^n)\right)/\epsilon, \tag{2.5}$$

and

$$H(s) = \begin{cases} 0 & , \quad s < 0 \\ \\ 1 & , \quad s \geq 0. \end{cases} \tag{2.6}$$

These equations hold for $1 \leq m \leq M$ and

$$x_{M+1}^{n+1} = x_1^{n+1} + l. \tag{2.7}$$

Throughout, we assume that

$$0 \leq \Delta t V_1'(L) \leq 1/2 \ \text{ and } \ 0 \leq \Delta t/\epsilon \leq 1/2.^1 \tag{2.8}$$

Theorem 1 Suppose (2.8) holds and that for $1 \leq m \leq M$

$$L \leq x_{m+1}^n - x_m^n \ \text{ and } \ 0 \leq u_m^n \leq V_1(x_{m+1}^n - x_m^n). \tag{2.9}$$

Then (2.9) holds for n replaced by $n+1$. ■

Proof. The identities (2.1) - (2.6) imply that

$$\bar{\gamma}_m^{n+1} = \bar{\gamma}_m^n + \Delta t\left(\bar{u}_{m+1}^n - \bar{u}_m^n\right) \tag{2.10}$$

and

$$\begin{aligned} \bar{u}_m^{n+1} = \ & V_1\left(\bar{\gamma}_m^{n+1}\right) + \left(\bar{u}_m^n - V_1\left(\bar{\gamma}_m^n\right)\right)(1 - \Delta t/\epsilon) \\ & + \left(V_2 - V_1\right)\left(\bar{\gamma}_m^n\right) H\left(\bar{\rho}_m^n - R\left(\bar{u}_m^n\right)\right)\Delta t/\epsilon \end{aligned} \tag{2.11}$$

[1] Recall, in section 1 we assumed $\Delta m = 1$ in order to obtain the follow-the-leader model. If, instead we had allowed any $0 < \Delta m$ our equations (2.2) and (2.3) would have been replaced by $\bar{\gamma}_m^{n+1} = \left(x_{m+1}^{n+1} - x_m^{n+1}\right)/\Delta m$ and $\bar{\rho}_m^{n+1} = \Delta m/\left(x_{m+1}^{n+1} - x_m^{n+1}\right)$. Our basic integration scheme (2.1) and (2.5) would be the same but $(2.8)_1$, would be modified to $\frac{\Delta t}{\Delta m} V_1'(L) \leq \frac{1}{2}$.

and the inequalities

$$\left.\begin{array}{l} L \le \bar{\gamma}_m^n \quad , \quad 1 \le m \le M \\ 0 \le \bar{u}_m^n = V_1\left(\bar{\gamma}_m^n\right) + \bar{\alpha}_m^n \ \text{ and } \ \bar{\alpha}_m^n \le 0 \ \ , \ \ 1 \le m \le M \end{array}\right\} \tag{2.12}$$

imply that

$$\bar{\gamma}_m^{n+1} \ge F\left(\bar{\gamma}_m^n\right) \stackrel{def}{=} \bar{\gamma}_m^n - \Delta t V_1\left(\bar{\gamma}_m^n\right). \tag{2.13}$$

The fact that Δt satisfies (2.8) implies that $F(\cdot)$ is monotone increasing on $[L, \infty)$ and thus (2.9) and (2.13) imply

$$\bar{\gamma}_m^{n+1} \ge F(L) = L \tag{2.14}$$

as desired. On the other hand the inequalities

$$\bar{u}_m^n - V_1\left(\bar{\gamma}_m^n\right) \le 0 \ \text{ and } \ \left(V_2 - V_1\right)\left(\bar{\gamma}_m^n\right) \le 0 \tag{2.15}$$

and (2.11) imply that

$$\bar{\alpha}_m^{n+1} = \bar{u}_m^{n+1} - V_1\left(\bar{\gamma}_m^{n+1}\right) \le 0. \tag{2.16}$$

The identity (2.11) when combined with (2.10) yields

$$\begin{array}{rl} \bar{u}_m^{n+1} & = (1 - \Delta t/\epsilon)\bar{u}_m^n + \left(V_1\left(\bar{\gamma}_m^n + \Delta t\left(\bar{u}_{m+1}^n - \bar{u}_m^n\right)\right) - V_1\left(\bar{\gamma}_m^n\right)\right) \\ & +(\Delta t/\epsilon)\left(1 - H\left(\bar{\rho}_m^n - R(\bar{u}_m^n)\right)\right) V_1(\bar{\gamma}_m^n) \\ & +(\Delta t/\epsilon) H\left(\bar{\rho}_m^n - R(\bar{u}_m^n)\right) V_2(\bar{\gamma}_m^n) \end{array} \tag{2.17}$$

or

$$\begin{array}{rl} \bar{u}_m^{n+1} & = \left(1 - \Delta t/\epsilon - \Delta t V_1'(\delta_m^n)\right)\bar{u}_m^n + \Delta t V_1'(\delta_m^n)\bar{u}_{m+1}^n \\ & +(\Delta t/\epsilon)(1 - H(\bar{\rho}_m^n - R(\bar{u}_m^n)))V_1(\bar{\gamma}_m^n) + (\Delta t/\epsilon)H(\bar{\rho}_m^n - R(\bar{u}_m^n))V_2(\bar{\gamma}_m^n), \end{array} \tag{2.18}$$

for some $\delta_m^n \ge \min\ (\gamma_m^{n+1}, \gamma_m^n) \ge L$ and (2.18) together with (2.6) and (2.8) and $u_m^n \ge 0,\ 1 \le m \le M$, implies that $\bar{u}_m^{n+1} \ge 0$. This conclude the proof of Theorem 1. ■

The estimates contained in Theorem 4.1 guarantee that the densities

$$\rho_m^n \stackrel{\text{def}}{=} \frac{1}{x_{m+1}^n - x_m^n}, \qquad 1 \le m \le M \tag{2.19}$$

satisfy

$$0 \le \rho_m^n \le \rho_{\max}. \tag{2.20}$$

These estimates further imply that the approximate solutions defined in (2.1) - (2.7) converge to solutions of the follow-the-leader model (1.20) - (1.22), (1.24), and (1.25) as $\Delta t \to 0^+$. This concludes Section 2.

3 Simulations

All computations in this section were run with the following equilibrium relations:

$$v_1(\rho) = v_1^\infty(1 - \rho/\rho_{\max}) \text{ and } v_2(\rho) = v_2^\infty(1 - \rho/\rho_{\max}). \tag{3.1}$$

These transform to

$$V_1(\gamma) = v_1^\infty \left(1 - \frac{L}{\gamma}\right) \text{ and } V_2(\gamma) = v_2^\infty \left(1 - \frac{L}{\gamma}\right) \tag{3.2}$$

where $L = \dfrac{1}{\rho_{\max}}$. The specific parameter used were

$$v_1^\infty = 100 \text{ feet/sec } = \frac{100 \times 3600}{5280} = 68.1818\ldots \text{ mph} \tag{3.3}$$

$$v_2^\infty = 40 \text{ feet/sec} = \frac{40 \times 3600}{5280} = 27.2727\ldots \text{ mph} \tag{3.4}$$

and

$$L = 15 \text{ feet}. \tag{3.5}$$

The latter number corresponds to a maximum car density of

$$\rho_{\max} = \frac{1}{15} \text{ cars/foot } = \frac{5280}{15} = 352 \text{ cars/mile}. \tag{3.6}$$

We used the constant switch curve introduced by Sopasakis [1]:

$$\gamma(u) = \gamma_* \quad , \quad 0 \leq u \tag{3.7}$$

with $\gamma_* = 20$ feet. For initial data we chose 3 sets of data:

$$x_m^{(k)}(0) = 20m + .1 \sin\left(\frac{km\pi}{200}\right) \tag{3.8}$$

for $-\infty \leq m \leq \infty$ and $k = 1, 2$, and 3. The observation that

$$x_{400}^{(k)}(0) = 8000 \text{ feet } = 1.5151\ldots \text{ miles} \tag{3.9}$$

and

$$x_{m+400}^{(k)}(0) = x_m^{(k)}(0) \tag{3.10}$$

implies we may interpret the data as initial data for a ring-road with 400 cars which is of length $1.5151\ldots$ miles. We chose constant initial velocities

$$u_m^{(k)}(0) = .5(V_1(\gamma_*) + V_2(\gamma_*)),\ 1 \leq m \leq 400 \tag{3.11}$$

or

$$u^{(k)}(0) = 17.5 \text{ feet/sec } = 11.931818\ldots \text{ mph},\ 1 \leq m \leq 400. \tag{3.12}$$

These data guarantee points on both sides of the switch curve. Simulations were run with relaxation times

$$\epsilon = 1, 2, 4, \text{ and } 8. \tag{3.13}$$

Below, we show the long-time spatially and temporarily periodic solutions at time $t = 2$ hours when $\epsilon = 8$ seconds. Figures 3, 4, and 5 correspond to the initial data indexed by $k = 1, 2$, and 3 respectively. At earlier times the solution indexed by each particular k had k discontinuities per period. This phenomena persisted to $t = 2$ hours for the solution indexed by $k = 2$ but the solution corresponding to the $k = 3$ converged, by $t = 2$ hours, to a solution with one discontinuity per period.

The first two frames in each figure are self-explanatory. In the third frame of each figure we plot the curve $m \to (\gamma_m = x_{m+1} - x_m, u_m)$. This curve is shown in black. The blue

curves are the equilibrium curves $\gamma \to (\gamma, V_1, (\gamma))$ and $\gamma \to (\gamma, V_2(\gamma))$ and the red curve is the image of $u \to (20, u)$. The red dot - o - is the image of (γ_1, u_1). Complete animations of all of these simulations may be found at //www.math.cmu.edu/∼plin/congestioon/. The discontinuities in the profiles propagate at the speed

$$c \simeq 227.6 \pm .1 \quad \text{cars/minute.} \tag{3.14}$$

An analysis of these solutions may be found in Section 4.

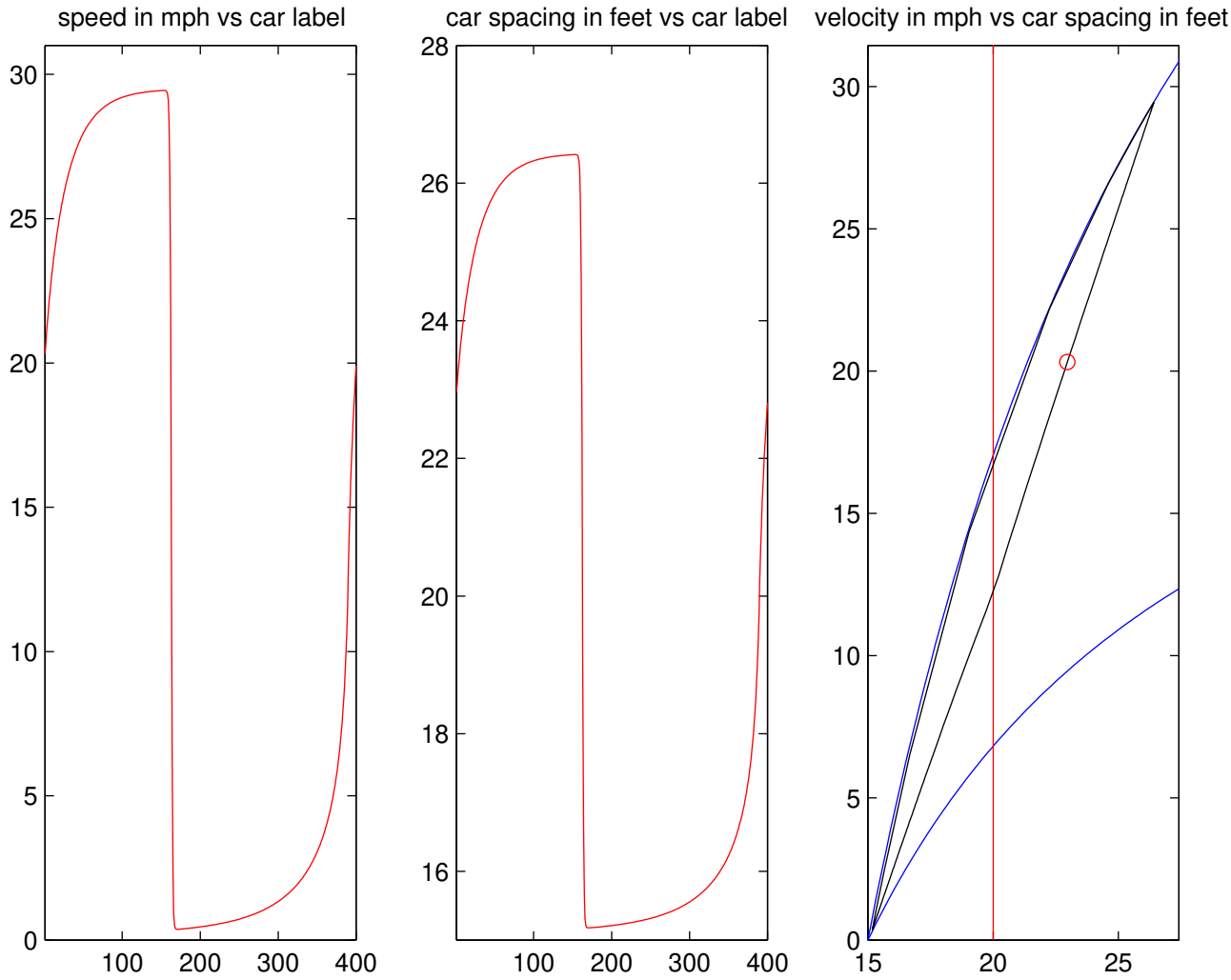

Figure 3

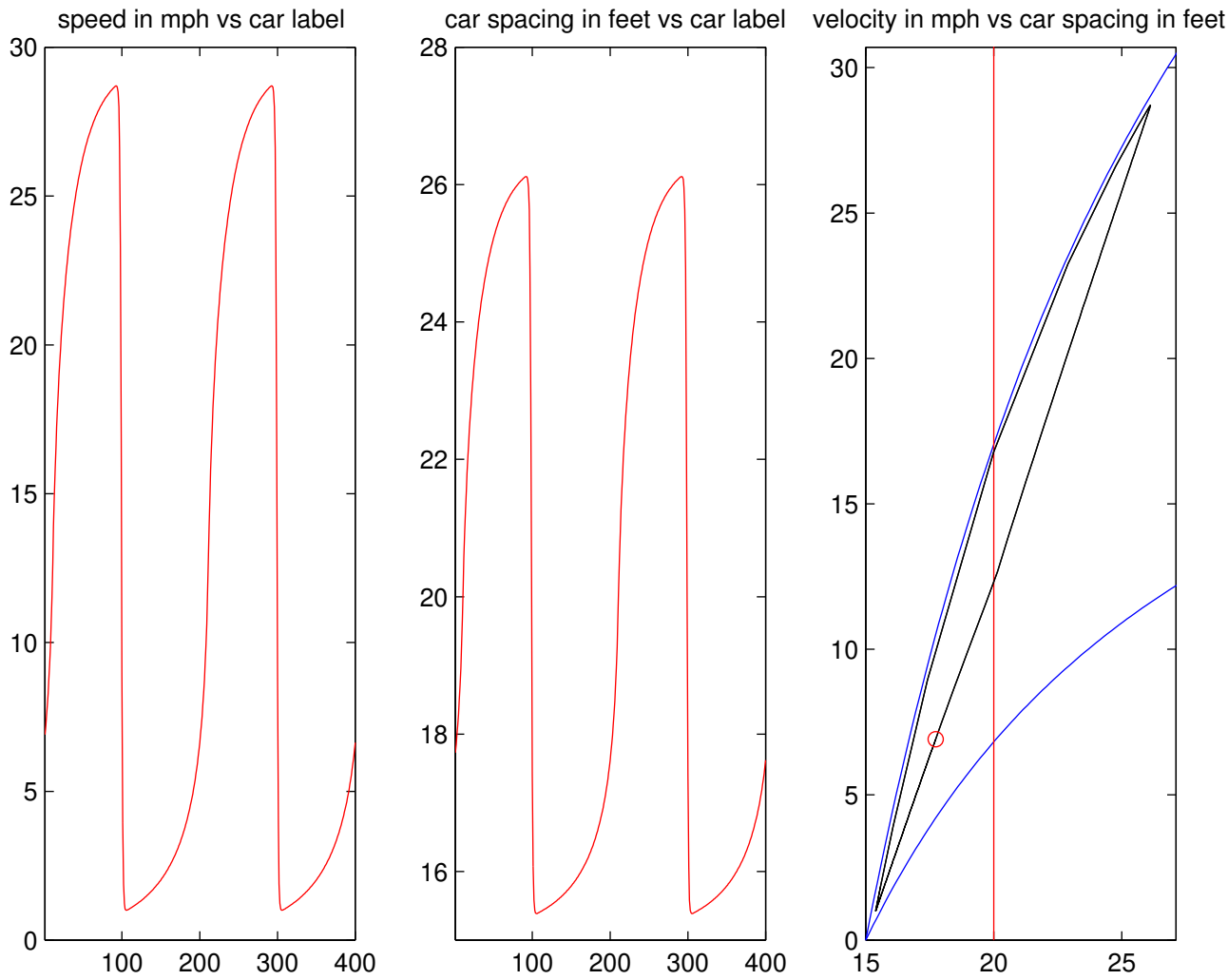
speed in mph vs car label
car spacing in feet vs car label
velocity in mph vs car spacing in feet
30
25
20
15
10
5
0
100
200
300
400
28
26
24
22
20
18
16
100
200
300
400
30
25
20
15
10
5
0
15
20
25

Figure 4

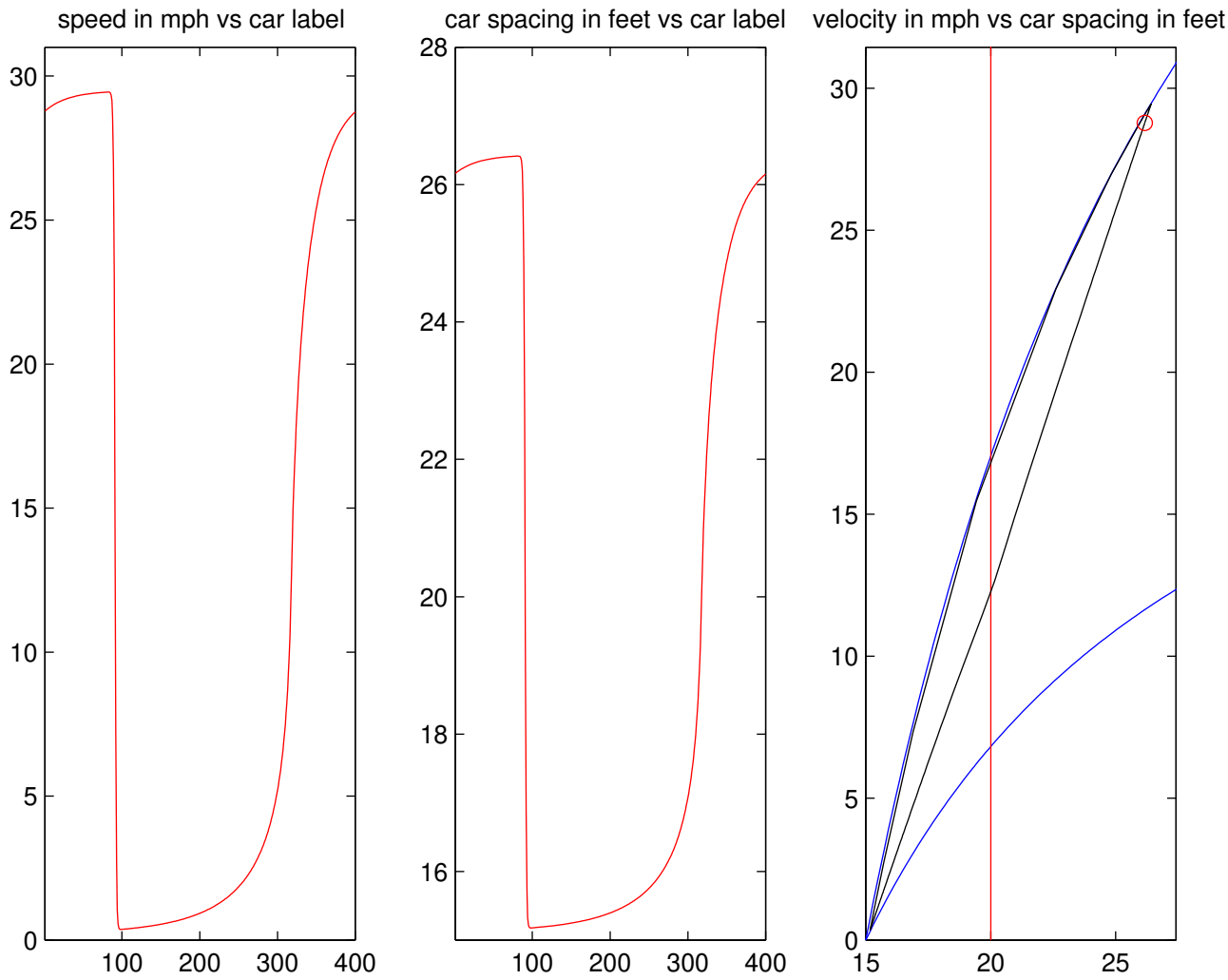

Figure 5

4 Travelling Waves

The wave trains obtained in section 3 are basically discrete approximations to travelling wave solutions to the continuum equations (1.9) - (1.19). In this section our goal is to show that the continuum system (1.9) - (1.19) actually supports such travelling waves. For definiteness we shall assume that the switch curve introduced in (1.4) is the one derived by Sopasakis in [1], namely the curve

$$R(u) = \rho_* \quad , \quad 0 \leq u. \tag{4.1}$$

With this choice of switch curve the Lagrangian equations become

$$\frac{\partial \bar{\gamma}}{\partial t} - \frac{\partial \bar{u}}{\partial m} = 0 \text{ and } \frac{\partial \bar{u}}{\partial t} - V_1'(\bar{\gamma})\frac{\partial \bar{u}}{\partial m} = \begin{cases} \dfrac{V_1(\bar{\gamma}) - \bar{u}}{\epsilon} & , \quad \bar{\gamma} > \gamma_* = \dfrac{1}{\rho_*} \\ \dfrac{V_2(\bar{\gamma}) - \bar{u}}{\epsilon} & , \quad \bar{\gamma} \leq \gamma_* = \dfrac{1}{\rho_*}. \end{cases} \tag{4.2}$$

Once again

$$V_1(\bar{\gamma}) = v_1(1/\bar{\gamma}) \text{ and } V_2(\bar{\gamma}) = v_2(1/\bar{\gamma}) \tag{4.3}$$

and we assume that both V_1 and V_2 are increasing and concave on $[L, \infty)$ and satisfy

$$0 = V_2(L^+) = V_1(L^+) \text{ and } 0 < V_2^{(p)}(\bar{\gamma}) < V_1^{(p)}(\bar{\gamma}) \text{ for } L < \bar{\gamma} < \infty \text{ and } p = 0, 1 \tag{4.4}$$

and the limit relations

$$\lim_{\bar{\gamma} \to \infty} (v_i(\bar{\gamma}),\ v_i^{(p)}(\bar{\gamma})) = (v_i^\infty, 0),\ i \text{ and } p = 1, 2 \tag{4.5}$$

where $0 < v_2^\infty < v_1^\infty$. L is related to $\rho_{\max}$ by $L = 1/\rho_{\max}$.

We start by describing the portion of the wave trains where both $\bar{\gamma}$ and $\bar{u}$ are increasing in m. These solutions are functions of

$$\xi = m + ct \tag{4.6}$$

and smoothness of these profiles requires that

$$c = V_1'(\gamma_*) \tag{4.7}$$

where once again $\gamma_* = \dfrac{1}{\rho_*}$ (see (4.1)). Equation $(4.2)_1$, implies that

$$\bar{u} = u_* + V_1'(\gamma_*)(\bar{\gamma} - \gamma_*). \tag{4.8}$$

In what follows we let $\Gamma_* > L$ be the unique solution of

$$V_1'(\Gamma_*) = V_2'(L^+). \tag{4.9}$$

If $L < \gamma_* < \Gamma_*$, we let

$$\bar{U} = V_1'(\gamma_*)(\gamma_* - L) \tag{4.10}$$

and note that for $V_2(\gamma_*) < u_* < \bar{U}$ the equation

$$u_* + V_1'(\gamma_*)(\bar{\gamma} - \gamma_*) = V_2(\bar{\gamma}) \tag{4.11}$$

has a unique solution $L < \gamma_- < \gamma_*$ satisfying

$$V_1'(\gamma_*) > V_2'(\gamma_-). \tag{4.12}$$

On the other hand, if $\Gamma_* < \gamma_*$ we let $L < \gamma_l < \gamma_*$ be the unique solution of

$$V_2'(\gamma_l) = V_1'(\gamma_*)) \tag{4.13}$$

and

$$\bar{U} = V_1'(\gamma_*)(\gamma_* - \gamma_l) + V_2(\gamma_l) \tag{4.14}$$

and note that for $V_2(\gamma_*) < u_* < \bar{U}$ the equation (4.11) has a unique solution $\gamma_- \in (\gamma_l, \gamma_*)$ satisfying (4.12).

In what follows we assume the parameter u_* in (4.8) satisfies $V_2(\gamma_*) < u_* \leq \bar{U}$ where $\bar{U}$ is defined in (4.10) or (4.14) as appropriate.

We now note that $(4.2)_2$, when combined with (4.8), implies that the profile $\bar{\gamma}$ must satisfy

$$V_1'(\gamma_*)\left(V_1'(\gamma_*) - V_1'(\bar{\gamma})\right)\frac{d\bar{\gamma}}{d\xi} = \begin{cases} \dfrac{V_1(\bar{\gamma}) - u_* - V_1'(\gamma_*)(\bar{\gamma} - \gamma_*)}{\epsilon}, & \bar{\gamma} > \gamma_* \\ \dfrac{V_2(\bar{\gamma}) - u_* - V_1'(\gamma_*)(\bar{\gamma} - \gamma_*)}{\epsilon}, & \bar{\gamma} \leq \gamma_*. \end{cases} \tag{4.15}$$

We normalize the profile by insisting that

$$\bar{\gamma}(0) = \gamma_*. \tag{4.16}$$

Noting that sign $(V_1'(\gamma_*) - V_1(\bar{\gamma})) =$ sign $(\bar{\gamma} - \gamma_*)$, that

$$V_1(\bar{\gamma}) - u_* - V_1'(\gamma_*)(\bar{\gamma} - \gamma_*) > 0 \quad , \quad \gamma_* < \bar{\gamma} < \gamma_+ \tag{4.17}$$

where $\gamma_* < \gamma_+$ is the unique solution of

$$V_1(\gamma_+) - u_* - V_1'(\gamma_*)(\gamma_+ - \gamma_*) = 0, \tag{4.18}$$

and finally that

$$V_2(\bar{\gamma}) - u_* - V_1'(\gamma_*)(\bar{\gamma} - \gamma_*) < 0 \quad , \quad \gamma_- < \bar{\gamma} < \gamma_* \tag{4.19}$$

where γ_- is defined in (4.11) we see that (4.15) and (4.16) has a unique increasing solution defined on $(-\infty, \infty)$. For $\xi < 0$ the solution is given by the quadrature formula

$$\epsilon V_1'(\gamma_*) \int_{\bar{\gamma}(\xi)}^{\gamma_*} \frac{(V_1'(\eta) - V_1'(\gamma_*))d\eta}{(u_* + V_1'(\gamma_*)(\eta - \gamma_*) - V_2(\eta))} = -\xi \tag{4.20}$$

and for $\xi > 0$ the solution is given by

$$\epsilon V_1'(\gamma_*) \int_{\gamma_*}^{\bar{\gamma}(\xi)} \frac{(V_1'(\gamma_*) - V_1'(\eta))d\eta}{(V_1(\eta) - u_* - V_1'(\gamma_*)\eta - \gamma_*))} = \xi. \tag{4.21}$$

Periodic Profiles

For any $\bar{\gamma} \in (\gamma_-, \gamma_*)$, we let $\Gamma(\bar{\gamma}) > \gamma_*$ be the unique solution of

$$V_1(\Gamma(\bar{\gamma})) - u_* - V_1'(\gamma_*)(\Gamma(\bar{\gamma}) - \gamma_*) = V_1(\bar{\gamma}) - u_* - V_1'(\gamma_*)(\bar{\gamma} - \gamma_*) \tag{4.22}$$

and note that

$$\frac{d\Gamma(\bar{\gamma})}{d\bar{\gamma}} = \frac{(V_1'(\bar{\gamma}) - V_1'(\gamma_*))}{(V_1'(\Gamma(\bar{\gamma})) - V_1'(\gamma_*))} < 0. \tag{4.23}$$

We are now in a position to define the periodic wave trains. For $-|\xi_a| < \xi \leq 0$, $\bar{\gamma}(\xi)$ is given by (4.20) and $|\xi_a|$ is given by

$$\epsilon V_1'(\gamma_*) \int_{\bar{\gamma}_a}^{\gamma_*} \frac{(V_1'(\eta) - V_1'(\gamma_*))d\eta}{(u_* + V_1'(\gamma_*)(\eta - \gamma_*) - V_2(\eta))} \stackrel{def}{=} |\xi_a| \tag{4.24}$$

where $\gamma_- < \bar{\gamma}_a < \gamma_*$. For $0 \leq \xi \leq \xi_{\Gamma(\bar{\gamma}_a)}$, $\bar{\gamma}(\xi)$ is given by (4.21) and $\xi_{\Gamma(\bar{\gamma}_a)}$ is given by

$$\epsilon V_1'(\gamma_*) \int_{\gamma_*}^{\Gamma(\bar{\gamma}_a)} \frac{(V_1'(\gamma_*) - V_1'(\eta))d\eta}{(V_1(\eta) - u_* - V_1'(\gamma_*) * \eta - \gamma_*))} \stackrel{def}{=} \xi_{\Gamma(\bar{\gamma}_a)}. \tag{4.25}$$

We extend these solutions to all ξ via

$$\bar{\gamma}(\xi) = \bar{\gamma}(\xi + \xi_{\Gamma(\bar{\gamma}_a)} + |\xi_a|). \tag{4.26}$$

The extended solution is a proper weak solution to (4.2). The relations (4.8) and (4.22) imply that the Rankine-Hugoniot relations for (4.2) hold across the discontinuities

$$\xi = m + V_1'(\gamma_*)t = \xi_{\Gamma(\bar{\gamma}_a)} \pm n\left(\xi_{\Gamma(\bar{\gamma}_a)} + |\xi_a|\right), n = 0, 1, \dots \ . \tag{4.27}$$

(4.22) also implies that

$$V_1'(\bar{\gamma}_a) > V_1'(\gamma_*) = \frac{V_1(\Gamma(\bar{\gamma}_a)) - V_1(\bar{\gamma}_a)}{\bar{\Gamma}(\bar{\gamma}_a) - \bar{\gamma}_a} > V_1'(\Gamma(\bar{\gamma}_a)) \tag{4.28}$$

and thus across these discontinuities the Lax entropy condition is satisfied. Recalling that the particular solutions of interest to us must be M periodic, we see that (4.24) and (4.25) imply that for some integer $k \geq 1, \bar{\gamma}_a$ and u_* must be such that

$$k\epsilon V_1'(\gamma_*)\left[\int_{\bar{\gamma}_a}^{\gamma_*} \frac{(V_1'(\eta) - V_1'(\gamma_*))d\eta}{(u_* + V_1'(\gamma_*)(\eta - \gamma_*) - V_2(\eta))} + \int_{\gamma_*}^{\Gamma(\bar{\gamma}_a)} \frac{(V_1'(\gamma_*) - V_1'(\eta))d\eta}{(V_1(\eta) - u_* - V_1'(\gamma_*)(\eta - \gamma_*))}\right] = M. \tag{4.29}$$

The condition that $x(M,t) = x(1,t) + l$ implies that $\bar{\gamma}_a$ and u_* must also satisfy

$$k\epsilon V_1'(\gamma_*)\left[\int_{\bar{\gamma}_a}^{\gamma_*} \frac{(V_1'(\eta) - V_1'(\gamma_*))\eta d\eta}{(u_* + V_1'(\gamma_*)(\eta - \gamma_*) - V_2(\eta))} + \int_{\gamma_*}^{\Gamma(\bar{\gamma}_a)} \frac{(V_1'(\gamma_*) - V_1(\eta))\eta d\eta}{(V_1(\eta) - u_* - V_1'(\gamma_*)(\eta - \gamma_*))}\right] = l. \tag{4.30}$$

We conclude this section with an analysis of the equations (4.29) and (4.30). We first note that the integer $k \geq 1$ in these equations is equal to the number of discontinuities of $\bar{\gamma}(\cdot)$ per period. We also note that instead of using u_* and $\bar{\gamma}_a$ as our basic parameters we may instead use γ_- and $\bar{\gamma}_a$. With this choice

$$u_* + V_1'(\gamma_*)(\eta - \gamma_*) - V_2(\eta) = V_2(\gamma_-) - V_2(\eta) + V_1'(\gamma_*)(\eta - \gamma_-) \tag{4.31}$$

and for $\eta \simeq \gamma_-$ we have

$$u_* + V_1'(\gamma_*)(\eta - \gamma_*) - V_2(\eta) \simeq (V_1'(\gamma_*) - V_2'(\gamma_-))(\eta - \gamma_-). \tag{4.32}$$

The last identity, together with

$$V_1'(\eta) - V_1'(\gamma_*) \simeq |V_1''(\gamma_-)|(\gamma_* - \eta) \tag{4.33}$$

implies that

$$\begin{aligned} & k\epsilon V_1'(\gamma_*) \int_{\bar\gamma_a}^{\gamma_*} \frac{(V_1'(\eta) - V_1'(\gamma_*))d\eta}{(u_* + V_1'(\gamma_*)(\eta - \gamma_*) - V_2(\eta))} \\ & \simeq \frac{k\epsilon V_1'(\gamma_*)|V_1''(\gamma_*)|}{(V_1'(\gamma_*) - V_2'(\gamma_-))} \int_{\bar\gamma_a}^{\gamma_*} \frac{(\gamma_* - \eta)}{(\eta - \gamma_-)} d\eta \\ & = \frac{k\epsilon V_1'(\gamma_*)|V_1''(\gamma_*)|}{(V_1'(\gamma_*) - V_2'(\gamma_*))} \left[(\gamma_* - \gamma_-) ln \left(\frac{\gamma_* - \gamma_-}{\bar\gamma_a - \gamma_-} \right) - (\gamma_* - \bar\gamma_a) \right] \end{aligned} \tag{4.34}$$

and that

$$\begin{aligned} & k\epsilon V_1'(\gamma_*) \int_{\bar\gamma_a}^{\gamma_*} \frac{(V_1'(\eta) - V_1'(\gamma_*))\eta d\eta}{(u_* + V_1'(\gamma_*)(\eta - \gamma_*) - V_2(\eta))} \\ & \simeq \frac{k\epsilon V_1'(\gamma_*)|V_1''(\gamma_*)|}{(V_1'(\gamma_*) - V_2'(\gamma_-))} \left[\gamma_- \int_{\bar\gamma_a}^{\gamma_*} \frac{(\gamma_* - \eta)}{(\eta - \gamma_-)} d\eta + \frac{(\gamma_* - \bar\gamma_a)^2}{2} \right] \end{aligned} \tag{4.35}$$

for $\gamma_- < \bar\gamma_a \leq \gamma_*$. The asymptotic formulas (4.34) implies that for any $L \leq \gamma_- < \gamma_*$ so that $V_1'(\gamma_*) > V_2'(\gamma_-)$ there exists a $\bar\gamma_a(\gamma_-, \gamma_*) \in (\gamma_-, \gamma_*)$ such that (4.29) holds. With this choice of $\bar\gamma_a$, equation (4.30) reduces to

$$\begin{aligned} & k\epsilon V_1'(\gamma_*) \left[\int_{\bar\gamma_a(\gamma_-,\gamma_*)}^{\gamma_*} \frac{(V_1'(\eta) - V_1'(\gamma_*))(\eta - \gamma_-)d\eta}{(V_2(\gamma_-) - V_2(\eta) + V_1'(\gamma_*)(\eta - \gamma_-))} \right. \\ & \left. + \int_{\gamma_a}^{\Gamma(\bar\gamma_a(\gamma_-,\gamma_*))} \frac{(V_1(\gamma_*) - V_1(\eta))(\eta - \gamma_-)d\eta}{(V_1(\eta) - V_1(\gamma_*) + V_1'(\gamma_*)(\gamma_* - \eta))} \right] \\ & = l - M\gamma_- \end{aligned} \tag{4.36}$$

where $l - M\gamma_* \leq l - M\gamma_- \leq l - ML$. In the situation where $\gamma_* \geq \Gamma_*$ (see (4.9)) the asymptotic formula (4.35) guarantees that the left hand side of (4.36) diverges to plus infinity as $\gamma_- \to \gamma_l^+$ (see (4.13)) and that it converges to zero as $\gamma_- \to \gamma_*^-$ and thus if $\gamma_* \geq \Gamma_*$ and $l - M\gamma_* \geq 0$ we are guaranteed that (4.36) is solvable. When $\gamma_* < \Gamma_*$, solvability is guaranteed if $l - M\gamma_* \geq 0$ and $l - ML$ is in the range of the left hand side of (4.36).

References

[1] Sopasakis, A., "Unstable Flow and Modeling," Mathematical and Computer Modeling (to appear).

[2] Aw, A. and Rascle, M., Resurrection of Second Order Models of Traffic Flow? *SIAM J. Appl. Math*, 60, 3, 916-938, (2000).

[3] Greenberg, J. M., Extensions and Amplifications of a Traffic Model of Aw and Rascle, *SIAM J. Appl. Math* (in press).

[4] Argall, B., Cheleskin, E., Greenberg, J. M., Hinde, C., and Lin, P. J., A Rigorous Treatment of a Follow-the-Leader Traffic Model with Traffic Lights Present, *SIAM J. Appl. Math* (submitted).

[5] Aw, A., Klar, A., Materne, T., and Rascle, M., Derivation of Continuum Traffic Flow Models from Microscopic Follow-the-Leader Models, *SIAM J. Appl. Math* (submitted).

[6] Kerner,B.S., Experimental features of self-organization in traffic flow, *Physical Review Letters*, 81, 3797, (1998).

[7] Kerner,B.S., Congested Traffic Flow, *Transp. Res. Rec.*, 1678, 160, (1998).